remote sensing

MDPI

Article

Validation of Four Satellite-Derived Soil Moisture Products Using Ground-Based In Situ Observations over Northern China

Weicheng Liu [1,2], Jixin Wang [1], Falei Xu [2], Chenrui Li [1] and Tao Xian [3,*]

[1] Lanzhou Central Meteorological Observatory, Lanzhou 730020, China; cnliuwc@163.com (W.L.); wangjix2015@163.com (J.W.); lcr0273@126.com (C.L.)
[2] College of Atmospheric Sciences, Lanzhou University, Lanzhou 730000, China; xufl20@lzu.edu.cn
[3] Department of Mechanics and Aerospace Engineering, Southern University of Science and Technology, Shenzhen 518055, China
* Correspondence: xiant@mail.ustc.edu.cn; Tel.: +86-153-4800-0490

Abstract: Accurately obtaining the spatial distribution of soil moisture and its variability are the basis for the land-atmosphere interaction study. We investigated the fidelity of four satellite-based soil moisture products (AMSR2, CCI, SMAP, and SMOS) using in situ observation during the period 2019–2020. The spatial distribution and variability of different soil moisture products in northern China were analyzed for different seasons and climate zones. The satellite products showed the best performance of summer soil moisture with the bias and uncertainty of the three products (CCI, SMAP, and SMOS) being less than 0.041 and 0.097, whereas soil moisture showed a large bias in winter. For all seasons, AMSR2 and CCI demonstrated a positive bias whereas SMAP and SMOS showed a negative bias. CCI product had little bias in spring, summer, and fall in northern China, while SMAP and SMOS had the smallest bias in winter. For different climate zones, CCI product performed better in describing the temporal variability of soil moisture in arid climate zones with the correlation coefficients > 0.50 for most areas, while AMSR2 product provided a similar spatial distribution. In the eastern monsoon region, the soil moisture from SMAP and SMOS was found to have a large bias, whereas the bias in CCI product was small. Four products failed to reproduce the observed soil moisture characteristics in the transitional zones affected by the summer monsoon, with a positive bias found in AMSR2 and CCI and the largest biases in SMAP and SMOS products. We also suggest several reasons for the bias and error in the satellite soil moisture products. These results have important implications for soil moisture studies over midlatitude regions.

Keywords: soil moisture; satellite observation; northern China; validation

check for updates

Citation: Liu, W.; Wang, J.; Xu, F.; Li, C.; Xian, T. Validation of Four Satellite-Derived Soil Moisture Products Using Ground-Based In Situ Observations over Northern China. *Remote Sens.* **2022**, *14*, 1419. https://doi.org/10.3390/rs14061419

Academic Editors: John J. Qu, Luca Brocca, Michael H. Cosh, Andreas Colliander and Xianjun Hao

Received: 28 January 2022
Accepted: 13 March 2022
Published: 15 March 2022

Publisher's Note: MDPI stays neutral with regard to jurisdictional claims in published maps and institutional affiliations.

Copyright: © 2022 by the authors. Licensee MDPI, Basel, Switzerland. This article is an open access article distributed under the terms and conditions of the Creative Commons Attribution (CC BY) license (https://creativecommons.org/licenses/by/4.0/).

1. Introduction

Soil moisture is one of the key variables in the physical and chemical processes of the Earth's atmospheric, hydrological and ecological cycles. It affects the occurrence and development of weather and climate processes through evaporation, plant growth, and transpiration, which makes it one of the essential initial conditions of the numerical weather forecasting system [1]. Therefore, accurately observing and estimating the spatial distribution of soil moisture and its variability are conducive to understanding the energy and hydrological cycle and improving the accuracy of temperature and precipitation forecasts.

The soil moisture is conventionally obtained from in situ observations. The spatial distribution of soil moisture varies greatly due to the diversity of soil types, land use, topography, land cover, and single-point observations cannot represent the distribution characteristics of soil moisture in a certain area due to the lack of understanding of the law of soil moisture change on larger spatial scales. Such lack of representation greatly restricts the observation of soil moisture on a large spatial scale [2–4]. Therefore, many areas in the world are still missing accurate data on soil moisture. Even in areas where observations have been carried out, the spatial distribution of soil moisture is still poor, and the time

series is limited, especially in remote areas of the world. All these have brought challenges to the study of regional or global soil moisture distribution and its variability. Therefore, it is gravely necessary to develop alternative data that can accurately describe the regional soil moisture distribution.

Remote sensing, especially satellite-based observation, can observe soil moisture over a larger area. According to different remote sensing measurements, soil moisture inversed from satellite observation can be classified into optical/thermal infrared remote sensing, active and passive microwave sensor remote sensing, each with its own advantages. The optical/thermal infrared remote-sensing method mainly uses the spectral reflectance characteristics of the soil surface, soil surface emissivity, and surface temperature to estimate soil moisture [5,6]. This method provides high spatial resolution, good availability of satellite sensors and hyperspectral data. However, the optical/thermal infrared remote sensing cannot penetrate clouds and vegetation canopy, with a maximum ground penetration depth of about 1 mm, which makes it sensitive to clouds, atmosphere, and vegetation.

The active microwave sensor remote-sensing method uses this feature to analyze the radar transmitting microwave beam and receive the signals reflected by the ground objects to indirectly obtain the soil moisture information of the ground surface [7,8]. In recent three decades, in-depth research has been carried out on the retrieval of soil moisture and the estimation of soil moisture based on microwave sensors, which is considered to be one of the most effective ways to obtain soil moisture information on a large spatial scale with a high temporal–spatial resolution [9]. The L-band radar has a better effect on soil moisture retrieval due to its better sensitivity to soil moisture. It has an advantage of a high spatial resolution, so that it can penetrate the surface depth of 5 cm, but is insensitive to clouds and atmosphere. However, it will be affected by vegetation and surface roughness and its temporal resolution is low. For example, the meteorological operational satellite MetOp of the European Meteorological Satellite Organization used its advanced microwave scatterometer ASCAT to provide soil moisture dataset, through which the soil moisture information with a 25–50 km horizontal resolution and 1–2 days' temporal resolution. The data provide a soil moisture estimation across Europe with a mean square root error of less than 0.06 $m^3 \cdot m^{-3}$ [10,11]. Based on the strong correlation between soil microwave radiation and soil moisture, the remote-sensing method of a passive microwave sensor uses a microwave radiometer to measure the microwave, brightness temperature emitted by the soil to achieve soil moisture retrieval. According to the number of retrieval parameters, it can be classified into single-value retrieval (soil moisture retrieval only) and multivalue retrieval (simultaneous retrieval of multiple parameters, such as soil moisture, vegetation volume ratio, vegetation moisture content, and other parameters). This method can detect soil moisture information with a surface depth of 5 cm. Being insensitive to clouds and atmosphere, it is capable of all-weather measurement, but it will be affected by vegetation and surface roughness, and the spatial resolution is slightly low. Passive microwave sensors have been installed on many satellites. This remote-sensing method is currently the fastest-growing soil-moisture-retrieving technology which yields a more complete dataset and is now widely used. For example, the Microwave Imager sensor of the Tropical Rainfall Measuring Mission (TRMM/TMI) can provide daily soil moisture information with a 0.125° horizontal resolution between 40° S and 40° N [12]. The Microwave Imaging Radiometer with Aperture Synthesis (MIRAS) of Soil Moisture and Ocean Salinity (SMOS) Earth Explorer Opportunity Mission of the European Space Agency (ESA) can provide soil moisture information with a 0.25° horizontal resolution over the globe and a 1 to 3 days' temporal resolution. The mean square root errors of SMOS soil moisture estimations of Europe, Africa, Oceania, and other regions are between 0.03~0.09 $m^3 \cdot m^{-3}$ [13,14]. The Advanced Microwave Scanning Radiometer for EOS sensor (AMSR-E) onboard the National Aeronautics and Space Administration (NASA) Aqua Satellite can provide daily soil moisture information with a 0.25° horizontal resolution over the globe, with the mean square root errors of soil moisture estimations of the Americas and Oceania between 0.03~0.10 $m^3 \cdot m^{-3}$ [15,16]. Recently, the Climate Change Initiative (CCI)

project, which is funded by the European Space Agency, has released a soil moisture dataset combined from multiple passive and active microwave remote-sensing satellites [11], which spans a 43-year period from late 1978 to the present. This long-term dataset has been widely validated and used in soil moisture studies [17–19].

The satellite-based soil-moisture-retrieval algorithm establishes a link between the remotely sensed microwave observation data with the soil moisture value. However, the use of different data-processing algorithms and transmission models during the retrieval, as well as some other influencing factors (e.g., the cloud amounts, the soil types and vegetation coverage, the surface roughness, and the uncertainty related to vegetation parameterization), will result in a variety of deviations in the products [20]. If these products with large bias and uncertainty are used in weather forecasts and climate predictions, the forecast results cannot provide reasonable fidelity. For example, Yuan et al. [21] used in situ observations and three soil moisture datasets derived from satellite observations to discuss the respective sensitivity of the convection initiation to soil moisture in the central United States. The results, based on in situ observation, show that convective activity in the afternoon often occurs in dry soil. However, this conclusion is not remarkable when adapting the satellite products, the sign (positive feedback or negative feedback) and intensity of the influence of soil moisture on convective activity vary among datasets. Helgert and Khodayar [22] found that high-spatial-resolution products are adequate to express the variability of soil moisture, but they would also increase significant uncertainty. The results obtained using the retrieved products to discuss the relationship between soil moisture and convective precipitation may be different from those obtained using the field observation data. Therefore, it is of great importance to identify the characteristics of their temporal–spatial error when using or improving soil moisture retrieved products.

Located in the mid-to-high latitudes of Asia, northern regions of China demonstrate great differences in topography, landforms, vegetation types, and diverse climatic characteristics (Figure 1). Therefore, the discussion of the applicability of different soil-moisture-retrieved products in this area can further clarify the availability and limitations of different methods under different climates and underlying surface conditions, providing solid support for further improvement of the numerical model. Previous studies have evaluated the applicability of different soil moisture retrieved products in parts of northern China [23–26]. Existing research works have achieved many meaningful results, but most of them focused on the applicability of a single product, station, or a small area of soil moisture products and few pieces of research were carried out to evaluate the applicability of multiple retrieved products over a larger scale of areas in a comprehensive and systematic manner. Here, we used the daily observation data of soil moisture from 2019 to 2020 to assess the applicability of the latest satellite-retrieved soil moisture products in northern China, with a view to facilitating the rational use of satellite-derived soil moisture products under different climates and underlying surface conditions, and to provide references for the improvement of the remote-sensing retrieving algorithm.

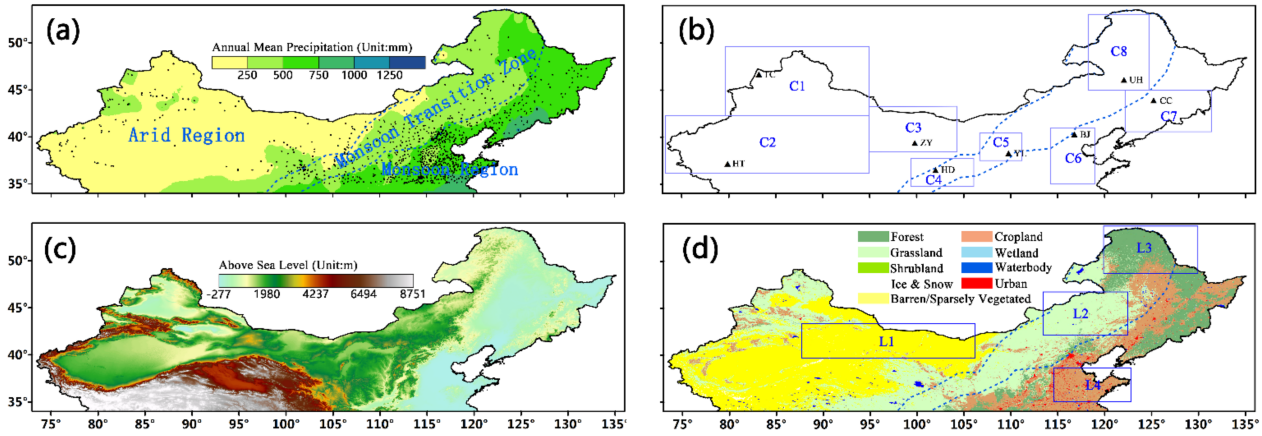

Figure 1. (**a**) Climate zones (separated by blue dashed lines) and in situ sites (black dots) in the study area. (**b**) Eight typical areas (blue rectangles) and the corresponding representative stations (black triangles). The zones C1 to C8 respectively represent northern Xinjiang, southern Xinjiang, Hexi Corridor, Qinghai–Tibet Plateau Slope, northern Loess Plateau, North China Plain, eastern Northeast Plain, and western Northeast Plain. The information of the representative stations is listed in Table 1. (**c**) The topography of the study area. (**d**) The distribution of vegetation type, with blue rectangles denoting different types: L1 as the Gobi desert, L2 as the grassland, L3 as the for-est, and L4 as the farmland.

2. Materials and Methods

2.1. The Study Area

The study area is the area north of 35° N in China, an area with diverse and complex topographic and subsurface conditions and a wide range of climate types. The distributions of the climate zones, topography and vegetation type in Northern China are shown in Figure 1.

There are three different climatic zones in this area according to the main influencing weather systems and the average annual precipitation. The eastern monsoon region (MR) is located in the North China Plain and the eastern part of the Northeast Plain of China (Figure 1c), characterizing as a temperate humid and semihumid continental monsoon climate. The rain belt in summer is mainly controlled by the East Asian summer monsoon, with most areas receiving average annual precipitation of 400–800 mm (Figure 1a). The western arid region (AR) is covering most parts of northwestern China and western Inner Mongolia. The AR is less affected by the summer monsoon due to its inland location, resulting in an arid climate (annual precipitation < 250 mm) and deserts and desert grasslands coverage (Figure 1d). The monsoon transition zone (MTZ) is alternatively affected by the Asian monsoon or the westerly zone in different seasons. The cold–dry and warm–humid air masses frequently intersect in the MTZ, resulting in annual precipitation of about 250–500 mm (Figure 1a) and diverse vegetation conditions and soil moisture.

To examine the fidelity of satellite soil moisture products in different climate zones, 8 representative regions, jointly determines based on local climatic characteristics, topography and land cover, located in the 3 climate zones were used for analysis. The representative regions are divided as shown in the blue rectangles in Figure 1b, among which the northern Xinjiang (C1), southern Xinjiang (C2), and the Hexi Corridor (C3) represent the western arid region, the slope of Qinghai–Tibet Plateau (C4), the northern part of the Loess Plateau (C5) and the western Northeast Plain (C8) represent the monsoon transition zone, and the North China Plain (C6) and the eastern Northeast Plain (C7) represent the eastern monsoon region. In addition, based on topography, land cover, precipitation, climate characteristics and site level (corresponding to data quality), Beijing, Changchun, Tacheng, Hotan, Zhangye, Haidong, Yulin and Ulanhot are selected as representative sites of the 8 regions (Table 1).

Table 1. Information of Representative Stations in Different Climate Zones.

Station	Location	Climate Type/ Climate Zone	Mean Annual Precipitation
Beijing	39.80° N, 116.47° E, 32.5 m	MR/C6	524.0 mm
Changchun	43.90° N, 125.22° E, 238.5 m	MR/C7	585.6 mm
Tacheng	46.73° N, 83.00° E, 536.6 m	AR/C1	303.8 mm
Hotan	37.13° N, 79.93° E, 1374.9 m	AR/C2	68.7 mm
Zhangye	38.93° N, 100.43° E, 1484.1 m	AR/C3	151.6 mm
Haidong	36.50° N, 102.10° E, 2125.0 m	MTZ/C4	343.6 mm
Yulin	38.27° N, 109.78° E, 1157.8 m	MTZ/C5	415.0 mm
Ulanhot	46.08° N, 111.05° E, 276.0 m	MTZ/C8	439.3 mm

2.2. Data Source

2.2.1. Satellite Observation Data Station Observation Data

Four newly released satellite-derived soil moisture datasets were analyzed, including AMSR2, CCI, SMAP, and SMOS soil moisture products. All products were obtained by the passive microwave sensor remote-sensing method.

Advanced Microwave Scanning Radiometer 2 (AMSR2) is onboard the Global Change Observation Mission-Water 1 (GCOMG-W1) satellite which was launched on 18 May 2012, and began to provide scientific data on 3 July 2012. AMSR2 inherits all frequency bands of AMSR-E from C-band (4 GHz–8 GHz) to X-band (8 GHz–12 GHz) and includes 2 other channels with a frequency of 7.3 GHz to minimize the Radio Frequency Interference (RFI) from the land area [27]. AMSR2 Level-3 daily soil moisture product, which were released by Japan Aerospace Exploration Agency, provide daily average soil moisture in the top soil surface layer of <1 cm thickness (units: volumetric water content $m^3 \cdot m^{-3}$) in low vegetation cover areas with a 25 km horizontal resolution and a target accuracy of $\pm 0.05\ m^3 \cdot m^{-3}$. AMSR2 datasets are available at https://suzaku.eorc.jaxa.jp/GCOM_W (accessed on 15 January 2022).

The Soil Moisture Active Passive (SMAP) satellite is an L-band (1.41 GHz) microwave observation satellite launched by NASA on 31 January 2015. It operates in a sun-synchronous twilight orbit with a revisit time of about 3 days. The main goal of the SMAP satellite is to provide global soil moisture and freeze/thaw state data. It combines a 3 km resolution radar (active microwave remote sensing) with a 36 km resolution microwave radiometer (passive microwave remote sensing). The radar stopped working on 7 July 2015, due to a technical failure, and thus SMAP product can only provide passive microwave observation data from that time [28,29]. This paper used daily soil moisture product (SMAP L3_SM_P) with a 36 km spatial resolution and surface layer depth from 0 to 5 cm. The datasets are available at https://nsidc.org/data/smap (accessed on 15 January 2022).

The Soil Moisture and Ocean Salinity (SMOS) satellite was launched by ESA on 2 November 2009, to detect the earth's soil moisture and ocean salinity. The only payload carried by the satellite is Microwave Imaging Radiometer using Aperture Synthesis (MIRAS). As the first space-based two-dimensional interferometer that operates in polar orbit and works at a central frequency of 1.413 GHz, MIRAS is capable of detecting L-band microwave radiation of the Earth's surface, and providing products with a spatial resolution of <50 km [30,31]. In this paper, the soil moisture products of SMOS-L3-SM were selected, including daily data with a 25 km spatial resolution and surface-layer depth from 0 to 5 cm. The datasets are available at https://www.catds.fr/sipad/ (accessed on 15 January 2022).

The European Space Agency (ESA)'s Climate Change Initiative (CCI) for soil moisture dataset is a combination of observation data of 10 different microwave sensors, such as TMI, AMSR, AMSR2, SMOS, SMAP, FY-3B, etc., with operating frequency ranging from 1.4 to 19.4 GHz. It produces an active-microwave-based-only product, a passive-microwave-based-only product and a combined active–passive product, which are sampled to global coverage of surface soil moisture at a spatial resolution of 0.25 degrees. It is the most comprehensive dataset in the world with wide coverage, long time series, and data

completeness [32,33]. This paper used the passive-microwave-based-only soil moisture product and the dataset version is v06.1. CCI datasets are available at https://catalogue.ceda.ac.uk/uuid/f5ffbd016e6b44858a33ae38ed2a149e (accessed on 15 January 2022).

2.2.2. In Situ Observation Data

The hourly soil volumetric water content provided by the China National Meteorological Information Center was used, including data from daily automatic weather stations in northern China from 2019 to 2020. This database has been comprehensively quality controlled and corrected for gross errors [34,35]. Due to the presence of frozen soil in the northern region in winter, the soil moisture observation instruments would stop working below 0 °C. Therefore, stations with a missing number of ≥20% were excluded from the observation series, and 1173 effective stations were finally obtained. The observation data included 20 depth layers (i.e., 0–10 cm, 10–20 cm, . . . , 190–200 cm) at intervals of 10 cm within a depth of 200 cm underground. Here only the top layer (i.e., 0–10 cm) is used to validate the satellite data.

The daily precipitation data observed by automatic weather stations from 2019 to 2020 at representative stations in 8 typical regions were used. The data were provided by the China National Meteorological Information Center (http://data.cma.cn, accessed on 15 January 2022).

2.3. Methodology

All the soil moisture products were expressed in terms of soil volumetric water content (unit: $m^3 \cdot m^{-3}$) for the consistency in dimensions. Quality control was first carried out on the observation data by removing the bad data with the soil volumetric water content values less than 0 $m^3 \cdot m^{-3}$ or higher than 1 $m^3 \cdot m^{-3}$. After obtaining all the satellite products, we checked the quality flag of each grid point value selected for interpolation to the station. Ultimately, data with a quality flag of "high" was selected for the analysis. Then, the inverse distance weighting interpolation was employed to interpolate the satellite data to the sites for further analysis. According to the horizontal resolution of each satellite product, the corresponding radius used for spatial matching is 25 km for AMSR2, CCI and SMOS, and 32.5 km for SMAP.

The median, probability distribution, and cumulative distribution function (CDF) of the time series distribution of soil moisture observations, and retrieved values were compared to qualitatively discuss the overall effect of soil moisture products [36], while Mean Deviation (BIAS), Mean Square Root Error (RMSE), and Correlation Coefficient (r) were used to quantitatively discuss the error distribution characteristics of soil moisture products [37]. Taylor charts bring correlation coefficient and standard deviation together to evaluate the overall performance of different soil moisture products [38]. When the Taylor distribution is drawn, the standard deviation and correlation coefficient of each site in different seasons are first calculated, and then the average distribution of the entire region is obtained. Therefore, it can be said that the Taylor distribution in the manuscript is the average state of the study area.

The calculation formulas involved are as follows:

$$BIAS = \frac{1}{n}\sum_{i}^{n}(Q_i - G_i)/G_i \times 100\% \quad (1)$$

$$RMSE = \left[\frac{1}{n}\sum_{i=1}^{n}(Q_i - G_i)^2\right]^{1/2} / \overline{G} \quad (2)$$

$$r = \frac{n\sum Q_i G_i - \sum Q_i \sum G_i}{\sqrt{\left[\sum Q_i^2 - (\sum Q_i)^2\right]\left[\sum G_i^2 - (\sum G_i)^2\right]}} \quad (3)$$

Among them, n is the total number of samples, i is the station sequence, G_i, Q_i and $\overline{G}$ are the in situ observation of soil moisture, the retrieved value of soil moisture satellite, and the average value of the in situ observation of soil moisture, respectively.

3. Results

3.1. Spatial Distribution Characteristics of Soil Moisture Products

Figure 2 shows the probability distribution of daily soil moisture observations from the in situ measurement and four satellite-based observation in northern China from 2019 to 2020. The in situ soil moisture values in most parts of northern China is below 0.50 $m^3 \cdot m^{-3}$, 97.3% of the stations have soil moisture values less than 0.40 $m^3 \cdot m^{-3}$, mainly ranging from 0.10 to 0.30 $m^3 \cdot m^{-3}$ (Figure 2a). The retrieved soil moisture values of AMSR2 are mostly below 0.80 $m^3 \cdot m^{-3}$, of which values ranging from 0.10 to 0.50 $m^3 \cdot m^{-3}$ account for about 90%, which are significantly overestimated compared to the in situ observation, especially for the area with soil moisture > 0.30 $m^3 \cdot m^{-3}$ (Figure 2b). The retrieved soil moisture values of CCI are concentrated between 0.10 and 0.40 $m^3 \cdot m^{-3}$, with an overestimation for the area $\leq$ 0.10 $m^3 \cdot m^{-3}$ and underestimation for the area > 0.40 $m^3 \cdot m^{-3}$. The probability distribution of soil-moisture retrieval of SMAP and SMOS is similar, where more than 90% of the soil moisture values are below 0.30 $m^3 \cdot m^{-3}$, of which values $\leq$ 0.20 $m^3 \cdot m^{-3}$ account for more than 85%, indicating significant underestimation compared to in situ observations. Zhuang et al. [39] also suggested that the SMOS soil moisture is lower based on their analysis of soil moisture distribution in China in 2012.

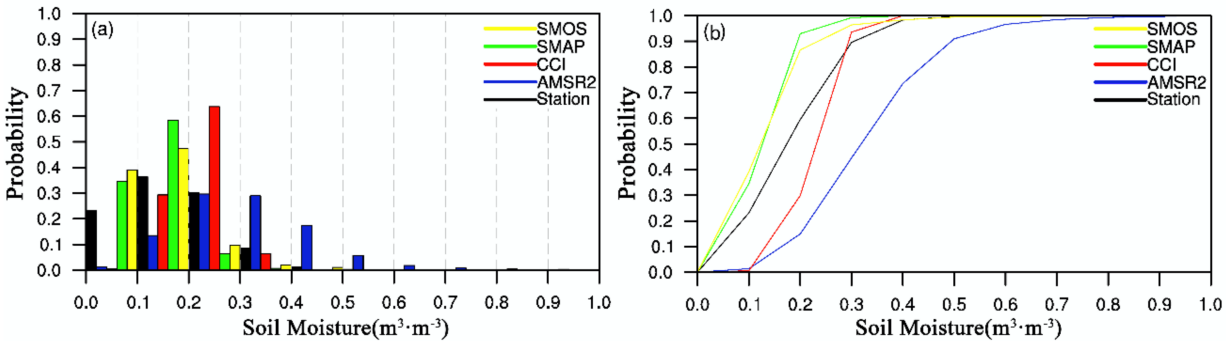

Figure 2. Probability distribution (**a**) and cumulative distribution function (**b**) of soil moisture observations and retrieved values of different soil moisture products.

Further analysis of the spatial distribution of the median of soil moisture from in situ and satellite observations is shown in Figure 3. There is a significant regional difference in the soil moisture. The areas with low soil moisture are located in the central part of northern China, primarily the northern Loess Plateau, northern North China Plain, and central Inner Mongolia Plateau with a median for most of these areas lesser than 0.20 $m^3 \cdot m^{-3}$. Areas with high soil moisture are located in the east of Northeast China, where has been significantly affected by monsoon activity. For satellite-derived products, AMSR2 can give the overall pattern of soil moisture distribution in northern China, with a better demonstration of the wet center of soil moisture, whereas the retrieved soil moisture is overall wetter, especially in the eastern monsoon region. SMAP and SMOS have better soil moisture retrieved results for the dry areas in the central and western parts of northern China, especially for the description of the dry center of soil moisture, but the retrieved results are mainly dry, especially dryer for the eastern monsoon region, and the degree of dryness is even greater for SMAP. CCI product has a similar distribution of soil moisture with the in situ observation with higher soil moisture in the monsoon region and lower in the rest, and can give the overall distribution pattern of soil moisture. The wet and dry centers are well described by CCI, and it can also describe the detailed characteristics of soil moisture distribution such as the areas of the Li River Valley, the northeastern slope of the Qinghai–Tibet Plateau and the Taihang Mountains. However, as with the probability

distribution, there is simulation bias towards wetness for drier soil areas and dryness for wetter soil areas.

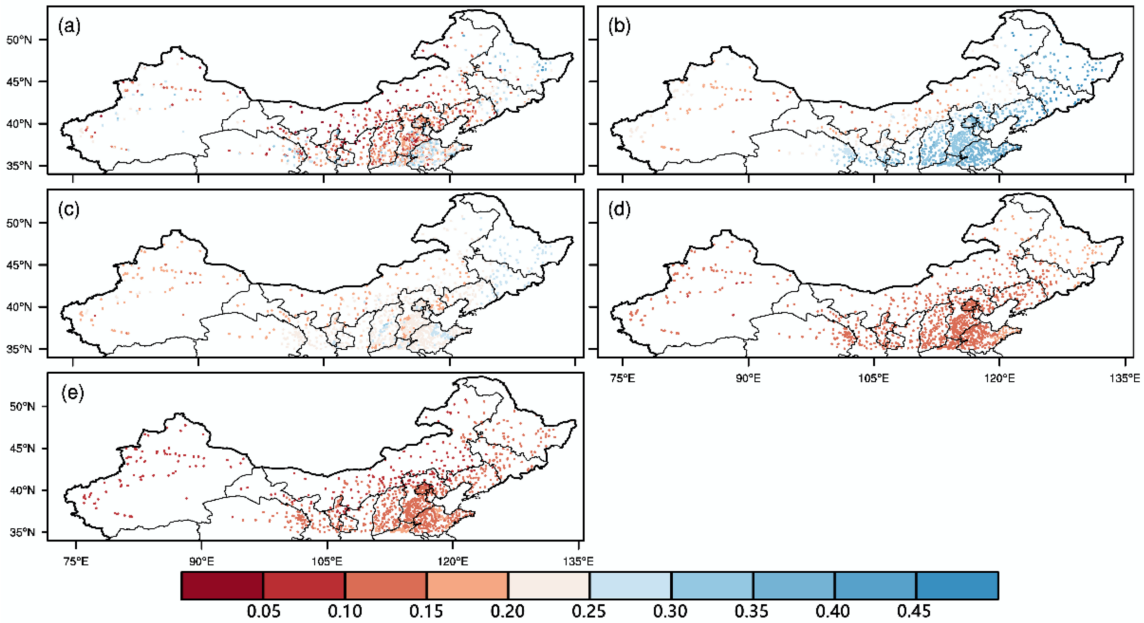

Figure 3. Soil moisture observation and spatial distribution of the median of different soil moisture products (Unit: $m^3 \cdot m^{-3}$); (**a**) Observation values; (**b**) AMSR2 product; (**c**) CCI product; (**d**) SMAP product; (**e**) SMOS product.

Figure 4 discusses the distribution of correlation coefficients between different retrieved soil moisture data and soil moisture observation data, and great differences among the products could be seen. Closed circles are statistically significant at the 99% confidence level, while the open ones are not. The correlation coefficients of AMSR2 show a positive correlation in the monsoon region and a negative correlation in the other regions. The positive correlation is dominant in the areas with wetter soil, with the strongest positive correlation occurring at the wet center of soil moisture ($r > 0.42$). For the drier areas, a negative correlation is dominant, exceeding 0.35 for the soil moisture dry center located in northern Hebei and central Inner Mongolia. The other three products are mainly positively correlated with the soil moisture observations, but the distribution patterns are quite different, with CCI product showing a significant positive correlation in the area east of 104° E, and the largest correlation coefficient among the three products, especially in the eastern foothills of the Taihang Mountains, the North China Plain and the Shandong Peninsula, where the correlation coefficients are >0.50 in most areas, but it is negative in parts of the Gobi Desert areas in the west. SMAP product shows basically positive correlations except for the weaker negative correlation in Shandong Peninsula and western Xinjiang, but the correlation coefficients are small (for most areas, $r < 0.30$). SMOS product has basically consistent positive correlation in the entire study area (except for the weaker negative correlation in the western Gobi Desert stations). In terms of correlation symbol, it has the best performance among the four products. Especially for areas in northern China, the eastern and western regions, and the eastern part of Northwest China, the retrieved products are better correlated with the observed values ($r > 0.38$ in most areas). Zhuang et al. [39] also obtained similar results stating that the correlation between SMOS product and observation exceeded 0.5 in Gansu, Beijing, Shaanxi, and Inner Mongolia in northern China. However, Zheng et al. [19] presented a negative correlation between AMSR-2 product and observation in the Shandian River Basin in northern China.

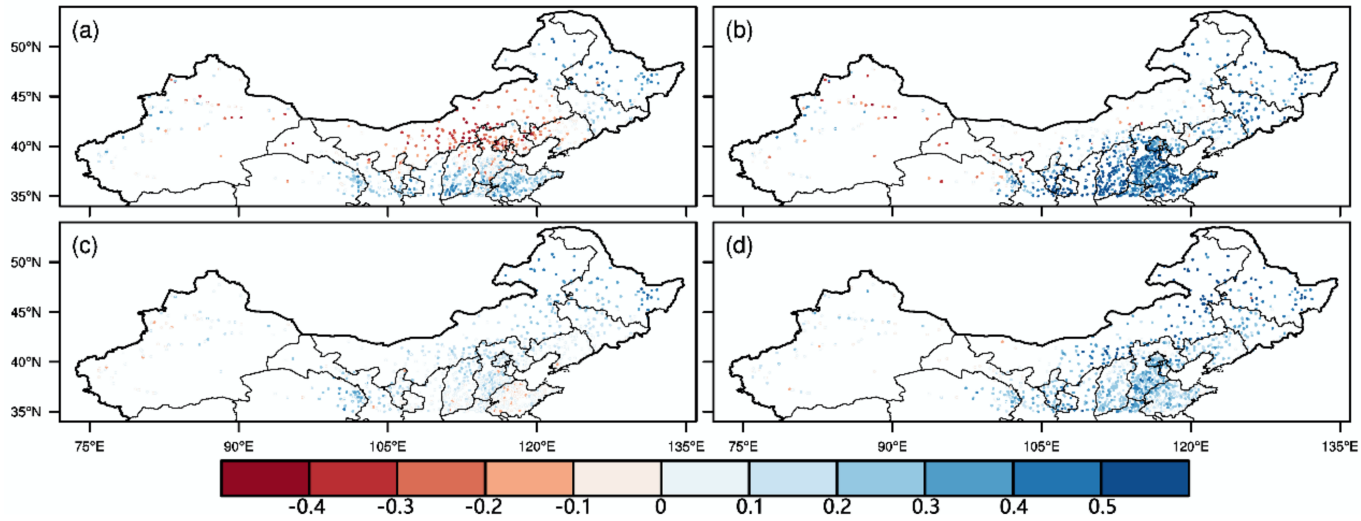

Figure 4. Spatial distribution of correlation coefficients between in situ and products derived from (**a**) AMSR2, (**b**) CCI, (**c**) SMAP, and (**d**) SMOS. Closed circles are statistically significant at the 99% confidence level, while the open ones are not.

Figure 5 shows the BIAS and RMSE spatial distributions of different soil moisture retrieved products to further quantify their performance. It can be seen that AMSR2 product shows underestimation for the central and southern parts of Xinjiang, while the rest of the regions are mainly overestimated, especially for the Loess Plateau and Northern China. The overestimation for most areas is >0.20 $m^3 \cdot m^{-3}$ higher than observations. The CCI product is better. When compared with observations, except for the obvious underestimation of most of Xinjiang and eastern Northeast China (underestimation is more than 0.10 $m^3 \cdot m^{-3}$), all the other regions have mainly smaller deviations, performing the best retrieving effect among the 4 products. SMAP and SMOS basically show relatively consistent error distribution characteristics, and in most areas of northern China, a smaller degree of overestimation is dominant (overestimation for most areas were <0.05 $m^3 \cdot m^{-3}$) and most of the other areas show underestimation, especially for Xinjiang, the slopes of the Qinghai–Tibet Plateau, the Shandong Peninsula and Northeast China.

The RMSEs of the four products are larger for Northern China and the eastern part of Qinghai. Among them, the RMSEs of the AMSR2 product are the largest, with greater retrieving error for the area east of 104° E, while for Xinjiang and Hexi Corridor areas, the RMSEs are relatively small. The spatial distribution pattern of the RMSE of the CCI product is similar to that of AMSR2, but its RMSE is smaller than that of AMSR2. SMAP and SMOS products show consistent RMSE distribution, with larger RMSEs in eastern Qinghai, Ili River Valley in Xinjiang, and central Northern China. The magnitudes of BIAS and RMSE are in good agreement with previous studies focusing on China [18,20]. Moreover, the BIAS and RMSE magnitudes of the AMSR2, CCI, SMAP, and SMOS products in northern China are comparable with those in the United States [18].

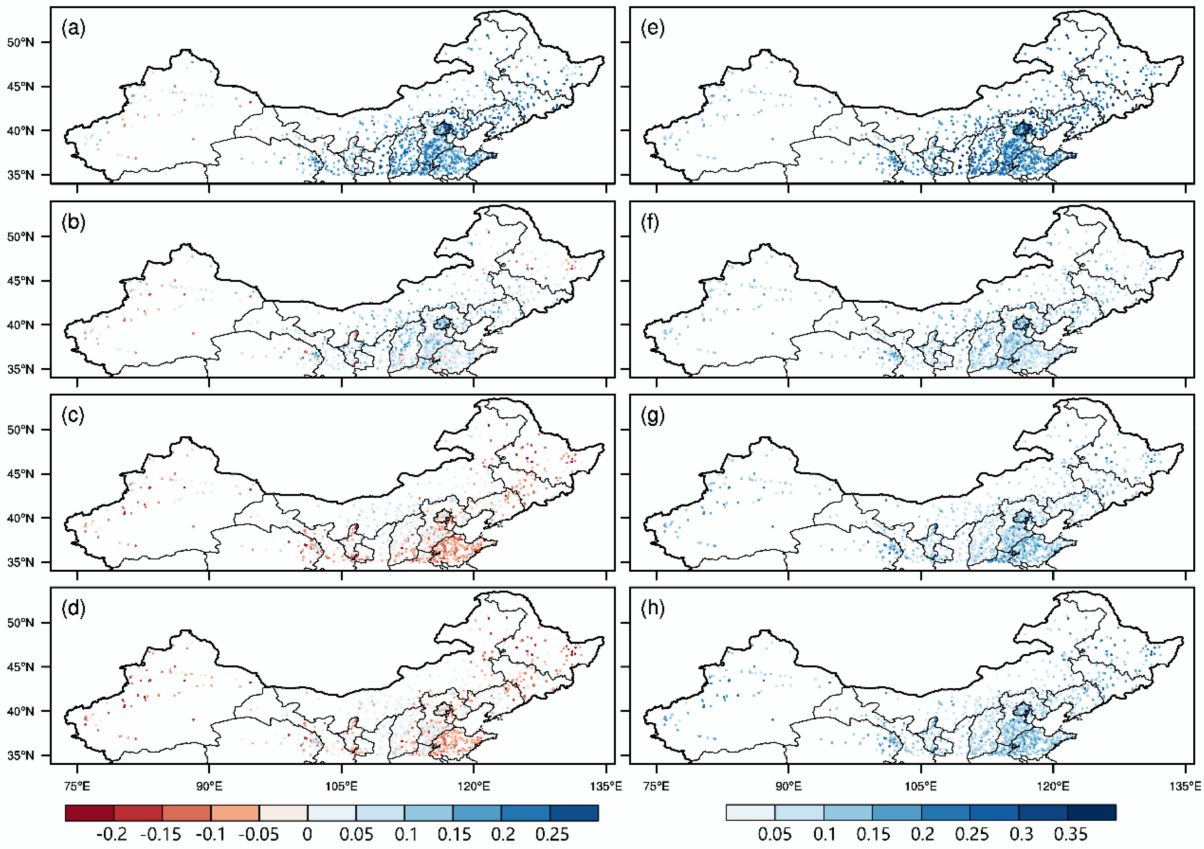

Figure 5. Spatial distributions of (left) BIAS and (right) RMSE of different soil moisture products (Unit: $m^3 \cdot m^{-3}$). (**a**,**e**) are AMSR2 product distribution, (**b**,**f**) are CCI product distribution, (**c**,**g**) are SMAP product distribution, (**d**,**h**) are SMOS product distribution.

3.2. Retrieval Deviation of Soil Moisture Products in Different Seasons

Based on comparing the retrieval effects of four soil moisture products in spring, summer, autumn, and winter, their applicability in different seasons in northern China can be immediately derived. The seasons were divided based on the meteorological definitions [40], namely spring (March to May), summer (June to August), autumn (September to November), and winter (December, January, February).

Table 2 lists the estimation deviations of different soil moisture products in spring, summer, autumn, and winter. The analysis shows that AMSR2 and CCI have positive estimation deviations for all seasons, and SMAP and SMOS have negative estimation deviations for all the seasons. In terms of different seasons, summer soil moisture is best described by all products. Most products have the smallest BIAS and RMSE in summer, while the description of winter soil moisture is poor. AMSR2 and CCI have the worst performance in winter among all seasons. In general, CCI has the best ability to characterize soil moisture in spring, summer, and autumn in northern China, with the smallest BIAS and RMSE among the four products. In winter, the BIAS of SMAP product is the smallest and the SMOS product has the smallest RMSE. It is worth noting that regardless of the seasons, the BIAS and RMSE of AMSR2 products are the largest among the four products, and significantly larger than those of the other products.

Table 2. Retrieval deviations of soil moisture products in different seasons (Unit: $m^3 \cdot m^{-3}$).

		AMSR2	CCI	SMAP	SMOS
Spring	BIAS	0.128	0.035	−0.044	−0.056
	RMSE	0.160	0.085	0.089	0.096
Summer	BIAS	0.077	0.026	−0.041	−0.035
	RMSE	0.121	0.085	0.097	0.095
Autumn	BIAS	0.167	0.042	−0.056	−0.045
	RMSE	0.196	0.086	0.094	0.089
Winter	BIAS	0.245	0.084	−0.036	−0.068
	RMSE	0.264	0.110	0.101	0.092

Figure 6 further shows the median spatial distribution of the observed values of soil moisture in different seasons and the four soil-moisture-retrieved values. For spring, summer, and autumn, except for the east of Northeast China, Ili River Valley in Xinjiang, and the east of Qinghai, the soil moisture is relatively high (>0.30 $m^3 \cdot m^{-3}$), and the rest of the regions all show relatively dry characteristics. AMSR2 product demonstrates a relatively consistent distribution pattern of soil moisture. However, the overestimation in the eastern monsoon region remains. SMAP and SMOS show mainly overestimation in central and eastern Inner Mongolia, while for the rest of the regions they are mainly underestimated. CCI product shows a more reasonable soil moisture distribution in this season, with a wetter soil over eastern Northeast China and eastern Qinghai, but there is still an overestimation of dry soil areas and an underestimation of wet soil areas. In winter, wetter soil areas in northern China are mainly distributed in Northeast China, Shandong Peninsula, the southern part of Northern China, the western part of the Loess Plateau, and the central–southern Xinjiang region, while the central part of Inner Mongolia and northern Xinjiang have lower soil moisture. AMSR2 product has better retrievals for the eastern part of Northeast China and the Shandong Peninsula. The rest of the regions are mainly overestimated with higher overestimation for the slopes of the Qinghai–Tibet Plateau and the central part of Inner Mongolia. SMAP and SMOS products show lower soil moisture ($\leq$0.30 $m^3 \cdot m^{-3}$) in the entire study area, and their ability to characterize soil moisture in this season is better. CCI can give the overall distribution pattern of dry soil areas and wet soil areas, but with a dominant overestimation for the dry areas.

Figure 7 shows the Taylor distribution of retrieved soil moisture products in different seasons. It can be seen that in all four seasons, the standard deviation is larger for AMSR2 product, and small for the other three products, with the smallest for SMOS product. In terms of correlation coefficients, the correlation coefficients between different soil moisture products and observed values in the four seasons are all less than 0.50. Relatively speaking, the correlation coefficient between CCI product and in situ observation is relatively stable. The correlation coefficients of SMOS and CCI are relatively large in spring, while the AMSR2 and CCI have relatively large correlation coefficients in summer and autumn. The CCI and SMAP products are relatively well correlated with observations in winter, while AMSR2 product is relatively less correlated. The SMOS product is negatively correlated to the observations. These results are consistent with those found by Peng et al. [41].

In general, the retrieval deviations of soil moisture products are quite different according to different seasons. The CCI product has a better overall effect on soil moisture retrieval in spring, summer, and autumn. The four products perform poorly on representing the winter soil moisture, thus give a relatively low value for reference.

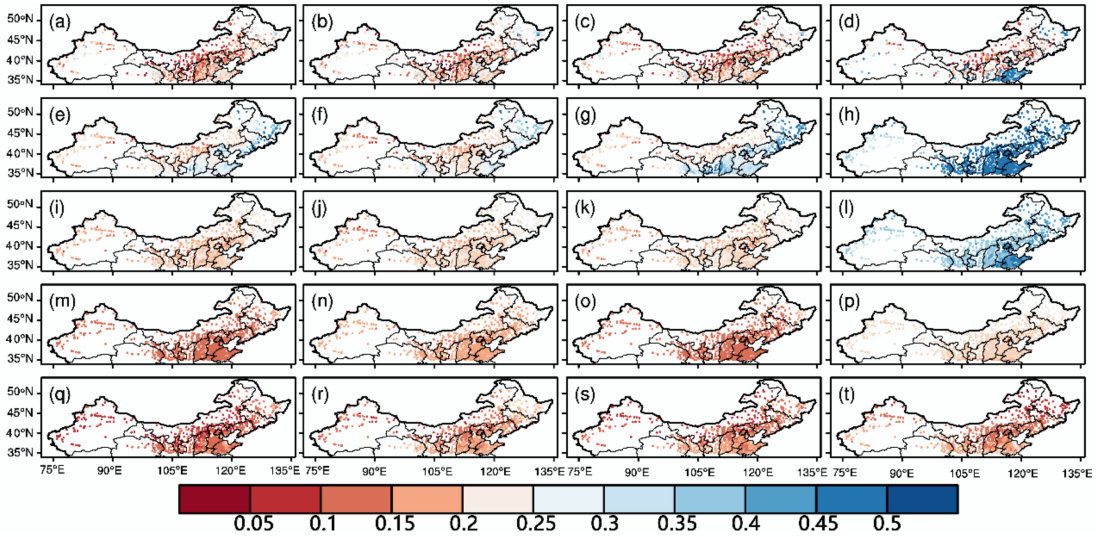

Figure 6. Spring (**a**,**e**,**i**,**m**,**q**), summer (**b**,**f**,**j**,**n**,**r**), autumn (**c**,**g**,**k**,**o**,**s**), and winter (**d**,**h**,**l**,**p**,**t**) Soil moisture observations and the median spatial distribution of different soil moisture products (Unit: $m^3 \cdot m^{-3}$). (**a**–**d**)—observation; (**e**–**h**)—AMSR2 product; (**i**–**l**)—CCI product; (**m**–**p**)—SMAP product; (**q**–**t**)—SMOS product.

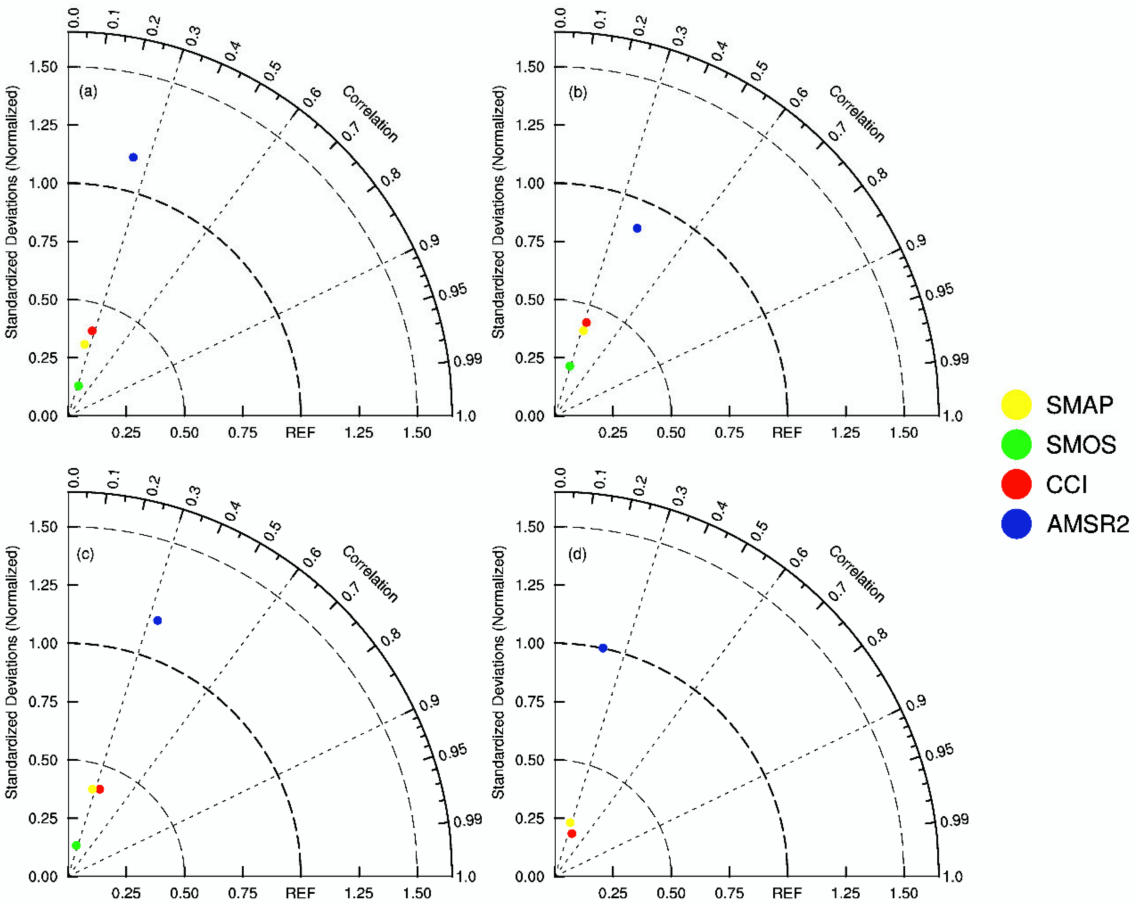

Figure 7. Taylor diagrams of soil moisture products in different seasons: (**a**) spring; (**b**) summer; (**c**) autumn; (**d**) winter.

3.3. Retrieval Deviation of Soil Moisture Products in Different Climate Zones

The deviation distributions of soil moisture products in 8 representative regions were compared and analyzed to further examine the ability of satellite products to characterize soil moisture in different climate zones. Figure 8 shows the distribution of the regional average box plots of daily soil moisture observations and retrieved values of stations in 8 regions from 2019 to 2020. It can be seen that the degree of concentration of soil moisture time series varies greatly among different regions. In the Hexi Corridor and western Northeast China, the degree of regional concentration is relatively high, while there is a relatively large dispersion in northern Xinjiang and the eastern part of Northeast China. For different soil moisture products, SMAP and SMOS have the highest degree of concentration, with all retrieved values tending to be average and therefore poor reference values. The degree of concentration of CCI product is the second largest, while the data of AMSR2 fluctuate greatly and have a small degree of concentration. In terms of different climate zones, the temporal variation of soil moisture is not well described by different products in arid climate zones. CCI product has relatively good retrieval effects on the median soil moisture, and AMSR2 product describes the distribution interval of the data better. For the eastern monsoon region, AMSR2 is significantly overestimated, especially in the eastern part of Northeast China. CCI product still performs relatively well and the availability of SMAP and SMOS is poor. In the transitional zone affected by the summer monsoon, the availability of the four products in this area is poor. AMSR2 and CCI are mainly overestimated, especially in the western part of Northeast China, while the data dispersion of SMAP and SMOS products is the smallest in these three climate zones which fails to provide the temporal change characteristics of soil moisture.

Table 3 shows the average simulation deviation of different soil moisture products in 8 regions. It can be seen that AMSR2 and CCI have positive deviations except for southern Xinjiang, where both show negative deviation. SMAP and SMOS have negative deviations except for the positive deviation in the northern part of the Loess Plateau. For arid climate zones, CCI product has the best retrieval effect in Xinjiang, especially in northern Xinjiang (the bias is 0.001 $m^3 \cdot m^{-3}$) and SMAP has a better retrieval effect in the Hexi Corridor area. In the eastern monsoon region, AMSR2 and CCI product shows positive deviations and the CCI retrieval effect is significantly better than the other products, with retrieval RMSEs in the North China Plain and the eastern Northeast China at 0.093 $m^3 \cdot m^{-3}$ and 0.102 $m^3 \cdot m^{-3}$, respectively, which are significantly smaller than those of the other three products. For the transitional area affected by the summer monsoon, the retrieval effects of different products vary greatly. The four products show consistent overestimation characteristics for the northern part of the Loess Plateau. For the slopes of the Qinghai-Tibet Plateau and western Northeast China, there are characteristics of overestimation of AMSR2 and CCI and underestimation of SMAP and SMOS. SMOS has a better retrieval effect on the slopes of the northern Loess Plateau and Qinghai-Tibet Plateau, while SMAP has a better retrieval effect on western part of Northeast China. In addition, it is worth noting that the deviation of soil moisture retrieval of AMSR2 product is significantly larger in eight typical regions. The BIAS and RMSE of SMOS and SMAP in Hexi Corridor (C3) are comparable with Zhang et al. [25]. In the North China Plain, the BIAS of AMSR-2 and RMSE in SMAP and SMOS are one order higher than those results from Zheng et al. [19].

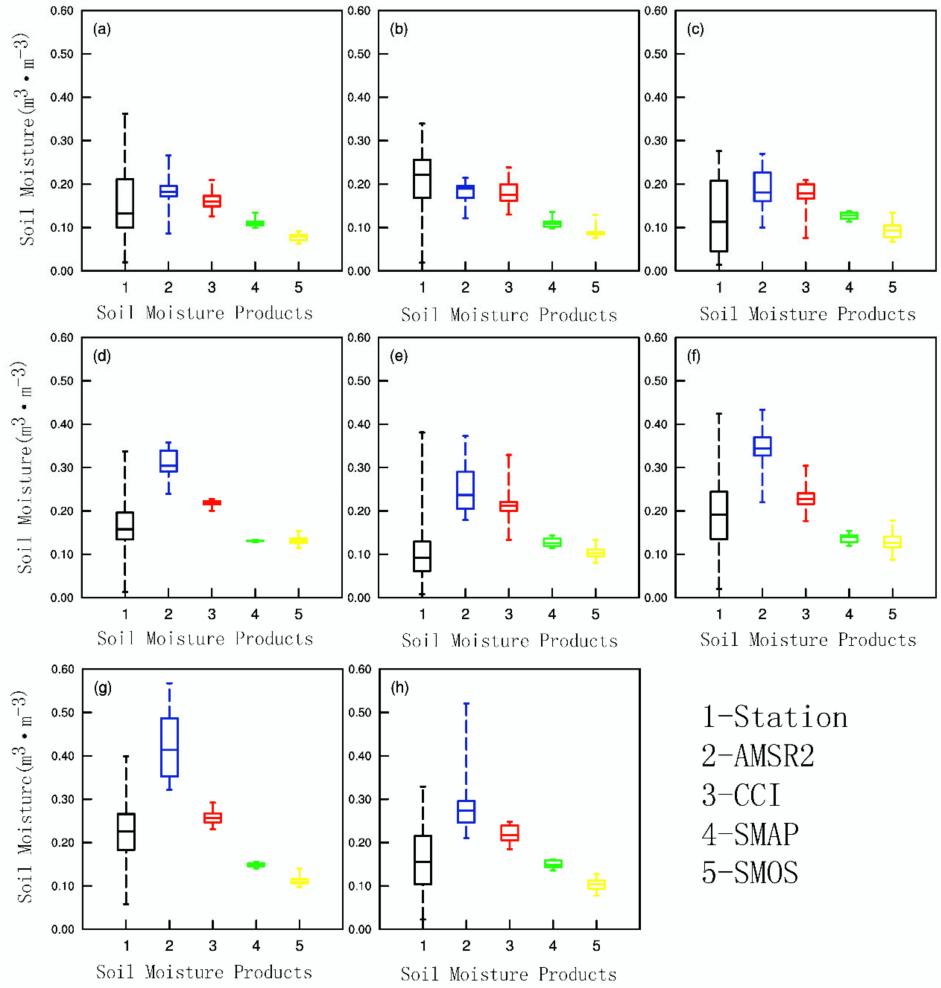

Figure 8. Box plots of average values of soil moisture observation and retrieval stations in representative regions (**a**) C1 (northern Xinjiang); (**b**) C2 (southern Xinjiang); (**c**) C3 (Hexi Corridor); (**d**) C4 (Qinghai–Tibet Plateau Slope); (**e**) C5 (northern Loess Plateau); (**f**) C6 (North China Plain); (**g**) C7 (eastern Northeast Plain); (**h**) C8 (western Northeast Plain).

Table 3. Retrieval deviations of soil moisture products in different climate zones (unit: $m^3 \cdot m^{-3}$).

		AMSR2	CCI	SMAP	SMOS
C1 (northern Xinjiang)	BIAS	0.021	0.001	−0.032	−0.073
	RMSE	0.111	0.107	0.113	0.123
C2 (southern Xinjiang)	BIAS	−0.046	−0.044	−0.096	−0.119
	RMSE	0.112	0.110	0.144	0.160
C3 (Hexi Corridor)	BIAS	0.063	0.043	−0.012	−0.026
	RMSE	0.128	0.108	0.107	0.105
C4 (Qinghai-Tibet Plateau Slope)	BIAS	0.151	0.101	0.013	0.006
	RMSE	0.196	0.134	0.095	0.092
C5 (northern Loess Plateau)	BIAS	0.164	0.054	−0.040	−0.002
	RMSE	0.196	0.107	0.101	0.097
C6 (North China Plain)	BIAS	0.158	0.040	−0.063	−0.053
	RMSE	0.194	0.093	0.115	0.118
C7 (eastern Northeast Plain)	BIAS	0.230	0.048	−0.078	−0.085
	RMSE	0.280	0.102	0.122	0.137
C8 (western Northeast Plain)	BIAS	0.133	0.048	−0.034	−0.059
	RMSE	0.175	0.104	0.098	0.109

Figure 9 shows the time series of daily soil moisture observations and estimated values of different soil moisture products at eight representative stations in different climate zones. It can be seen that the soil moisture in arid climate zones fluctuates greatly from day to day, especially in the desert areas stations Tacheng and Hotanlocating in the hinterland of Eurasia. For three stations (Zhangye, Tacheng, Hotan), SMAP and SMOS are better at describing the variability change characteristics of soil moisture, and SMAP has the best characterization ability for its estimated soil moisture, with variation amplitude of Zhangye station almost identical to that of the actual observation, but there is underestimation at Tacheng and Hotan stations. CCI and AMSR2 products have limited capabilities in depicting soil moisture in arid climate areas. They can only roughly give the soil moisture change characteristics of the Hotan station while the ability to estimate the soil moisture of the other stations is poor. For the eastern monsoon region, the characteristics of soil moisture variation are very different from those of arid regions, showing obvious characteristics of "longer duration of wetter soil and shorter duration of drier soil". AMSR2 has a poor characterization of the temporal variation of soil moisture at the Beijing station. The estimated time changes often appear in antiphase with the observations. CCI can demonstrate the fluctuations of soil moisture changes, but its fluctuation amplitude is smaller and overestimated compared to the actual observation. SMAP and SMOS have better estimation results for Beijing stations, and SMOS performs especially better. For Changchun station, all four products can basically reflect the temporal change trend of soil moisture, and CCI has the best performance, both for the dry–wet transition period of soil moisture or for the temporal variation fluctuation amplitude. AMSR2 product has an overestimation and the estimated change amplitude is stronger than the actual situation. SMAP and SMOS describe the temporal variation trend better, but there is a clear underestimation. In the transitional zone affected by the summer monsoon, the three stations show obvious continuous dryness and continuous wetter soils, which are basically characterized as "high soil moisture in the warm seasons and low soil moisture in the cold seasons". The periods of wetter soil at the Haidong station are concentrated between May and October each year, during which period all four products can give a good indication of the time change in soil moisture. Among them, SMOS has the best estimation effect for this station, providing estimated change trend and fluctuation amplitude basically consistent with the actual situation, while SMAP is the second best and AMSR2 can describe the soil dry–wet transition period, but with too large fluctuation amplitude and obvious overestimation. The fluctuation amplitude estimated by the CCI product is weaker than the actual situation. The soil at Yulin station is mainly dry all year round and the annual average soil moisture is <0.10 $m^3 \cdot m^{-3}$ with little variations. All four products have obvious overestimation at this station where AMSR2 has the largest overestimation. The time change trend of CCI product is basically the same as the actual situation, but the overestimation is about 0.06~0.14 $m^3 \cdot m^{-3}$ compared with the actual situation. SMOS and SMPA have the second-best estimation effect on the time change and AMSE2 has poor estimation effect. The soil moisture at Ulanhot station fluctuates slightly throughout the year and the period of wetter soil is shorter, mainly concentrated between June and August each year. For this station, AMSR2, SMPA, and SMOS describe the soil moisture time series well, but the estimated fluctuation amplitudes are obviously stronger than the actual situation. In particular, the daily soil moisture fluctuations of the AMSR2 product are more intense and significantly overestimated than the observations. The estimated soil moisture distribution range of the CCI product is very close to the actual situation, but its description of the duration of continuous dryness and wetness of the soil is not satisfactory (although the duration of wetness of soil is not much different from that of dryness).

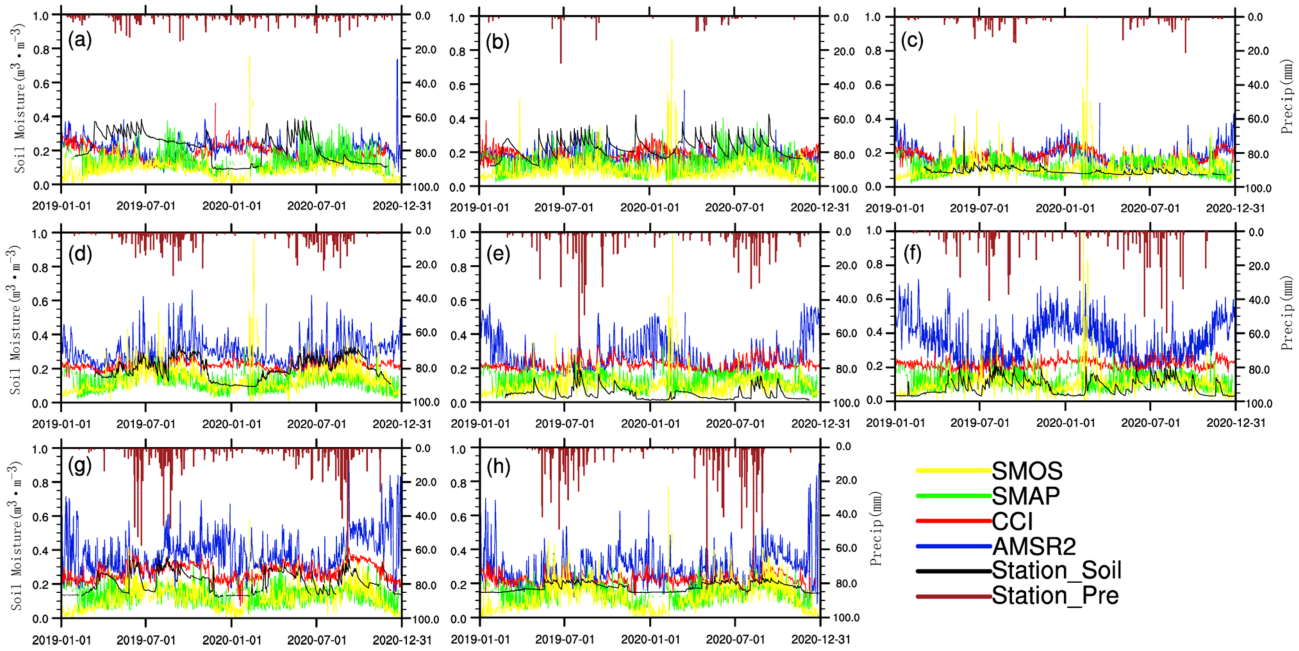

Figure 9. Time series of daily soil moisture (left ordinate axis, curve) and daily precipitation observations (right ordinate axis, histogram) observed and retrieved by eight representative stations in different climate zones. Panels (**a**–**h**) are data of stations Tacheng, Hotan, Zhangye, Haidong, Yulin, Beijing, Changchun and Ulanhot, respectively.

Generally speaking, different products have limited ability to characterize soil moisture in arid climate zones. SMAP and SMOS describe the trend of the soil moisture in this region well, while CCI and SMAP products have smaller estimation deviations for Xinjiang and the Hexi Corridor, respectively. For the eastern monsoon region, AMSR2 and CCI products are significantly overestimated, and the overall performance of CCI product is still relatively better than other products. SMAP and SMOS have better effects on soil moisture estimation in Northern China. In the transitional area affected by the summer monsoon, there are big differences among estimation effects of different products. SMOS has a better retrieval effect on the slopes of the Qinghai–Tibet Plateau. The temporal change trend of soil moisture in the northern part of the Loess Plateau estimated by CCI is consistent with the actual situation, while SMAP has a better retrieval effect on the western part of Northeast China.

4. Discussion

This study conducted a detailed analysis and evaluation of the applicability of the four latest satellite remote-sensing-retrieved soil moisture products in northern China. The results show that the CCI product has a better soil moisture retrieval capability in the region, while the remaining three products (especially SMAP and SMOS) are slightly insufficient in describing the soil moisture. These analyses also show that although satellite remote sensing could provide near-real-time observations and high-resolution soil moisture products, it is affected by many factors [42–44], resulting in great differences in the applicability of products in different regions. Therefore, it is very necessary to discuss the error sources of different retrieved products in order to carry out the further in-depth application of the products and improvement of the retrieval algorithm.

Four soil moisture products used in the study are all derived from passive microwave sensor remote-sensing data retrieval, so that RFI is an important factor that affects the effect of passive microwave remote sensing [45,46]. SMAP and SMOS use L-band sensors (the center frequency was 1.41 GHz). As is well known, the L-band will be affected by RFI generated by ground-based radar, resulting in contamination of satellite radar and microwave radiometer measurement data [47,48] and greater uncertainty in retrieved

results. Although the SMAP satellite installed the special frequency band filter which could eliminate part of the predetermined RFI spectrum [49,50], it still could not guarantee that all RFI received could be effectively eliminated. This may be one of the reasons for the poor retrieval effects of SMAP and SMOS products. The probability of the incidence of RFI in Asia is relatively high and the situation of RFI is even more serious. AMSR2 adopts C-band and X-band multi-frequency-channel observations. Especially with the help of two newly added observation channels with a frequency of 7.3 GHz compared with AMSR-E, observation data can be protected from RFI as much as possible [27]. CCI integrates the observation data of 14 different microwave sensors from multiple satellites. This fusion algorithm can effectively avoid or reduce RFI, making its retrieval effect better.

Vegetation coverage is one of the key factors that affect the estimation results of soil moisture, and the vegetation index is usually used as an indirect parameter for retrieval or correction of surface soil moisture [9,51]. Table 4 shows the estimation errors and correlation coefficients of soil moisture products in different land cover areas, which can further explore the applicability of different microwave sensors and different retrieval algorithms under different vegetation coverage conditions. It can be seen that the four products have large deviations in the estimation of soil moisture in areas with sparse vegetation coverage (the BIAS and RMSE are small because the soil moisture values in this type of area are originally small), and the correlations with the observed values are poor, AMSR2 and CCI in particular even show strong negative correlations with the observed values ($r < -0.20$), indicating insufficient estimation capabilities of the satellite retrieved products when applied to the Gobi Desert area. For grassland areas, the estimation capabilities of different retrieved products are obviously improved. SMOS and SMAP have better estimation capabilities for this type of uniform vegetation coverage area, with the correlation coefficients with the observed value at 0.423 and 0.205 respectively, which is largely consistent with the evaluation results of the two products in other regions of the world, i.e., the reliability of the two products in the more uniform land area is better [25,52]. For the uniform forest coverage area, the performance of the retrieved products is the same as that in the grassland areas, and the estimation effect is better than that in the grassland area, with correlation coefficients between the 4 products and observation data all exceeding 0.37, and the correlation coefficients between SMOS and the observed values approaching 0.57, which further confirm the better estimation effect of retrieved products for uniform land coverage areas. For farmland areas, the estimation deviations of different products are quite different. Among them, the estimation effect of CCI product, which merges multiple sensor data, is obviously better. This may be due to the strong seasonal variation of vegetation coverage and surface roughness in farmland areas and single sensor observation may not be able to effectively identify and extract the change characteristics of the underlying surface, while the merged multisource sensor-observation data may avoid the impact of changes in the underlying surface and build a corresponding correction plan based on the characteristics of the underlying surface climate change.

The depth of soil layer penetration and representative range of satellite remote sensing products may affect the accuracy of the retrieved results. The four satellite sensors used in the study are only capable of soil moisture retrieval on the surface of the land (depth $\leq$ 5 cm). Among them, the penetration depth of the C-band and X-band radiometers of the AMSR2 satellite is shallower (<2 cm). Even a small amount of vegetation coverage would significantly reduce the sensitivity of soil moisture retrieval, leading to higher errors in the estimation of soil moisture in vegetation areas [53–55]. The so-called "penetration" does not mean actively passing through the soil, but to calculate the depth of layer by analyzing the microwave signal emitted by the soil received by the satellite sensor. This calculation also has different bias depending on the difference in land coverage, land type, sensor sensitivity, etc., resulting in the estimated depth layer not necessarily reflecting the true situation. The in situ soil moisture data used in the study is the observation of soil moisture of the layer 0–10 cm underground, which has some deviations from the selected depth of layers of the four soil moisture retrieved products. This may be another factor that

led to larger deviations in the retrieved results and requires further consideration. Such factor is also one of the reasons that atmospheric reanalysis simulated soil moisture products are better than satellite-retrieved soil moisture products. At the same time, the soil moisture retrieved from satellites represents an average value of hundreds of km^2 (calculated with the 25–32 km spatial resolution of the satellite-derived products selected in the study), while the soil moisture is affected by factors such as precipitation, temperature, cloud cover, and topography which would result in very different spatial distributions [3,56]. Such spatial distribution varies even more so in the vast mountainous regions of northern China, such as the Taihang Mountain, the Yanshan Mountain, the Loess Plateau, the Tianshan Mountain, etc. This variation would lead to poor representativeness of the retrieval value of grid points and a large deviation from the station observations.

Table 4. Estimated errors and correlation coefficients of soil moisture products in different vegetation types.

Vegetation Types		AMSR2	CCI	SMAP	SMOS
L1 (Gobi desert)	BIAS	0.012	0.044	0.01	−0.027
	RMSE	0.131	0.117	0.106	0.102
	r	−0.245 *	−0.203 *	0.063 *	−0.033 *
	n	10,234	10,234	10,234	10,234
L2 (grassland)	BIAS	0.127	0.067	−0.001	−0.034
	RMSE	0.162	0.109	0.088	0.089
	r	−0.123 *	0.117 *	0.205 *	0.423 *
	n	26,316	26,316	26,316	26,316
L3 (forest)	BIAS	0.242	0.044	−0.054	−0.096
	RMSE	0.274	0.129	0.133	0.16
	r	0.374 *	0.432 *	0.402 *	0.569 *
	n	7310	7310	7310	7310
L4 (farmland)	BIAS	0.155	0.029	−0.076	−0.062
	RMSE	0.183	0.085	0.118	0.122
	r	0.136 *	0.388 *	0.025 *	0.196 *
	n	237,575	237,575	237,575	237,575

Note: * indicates that it has passed the $\alpha = 0.01$ significance test.

Precipitation is one of the main factors affecting the change in soil moisture. Analyzing the feedback of different soil moisture to precipitation can obtain the influence of wet and dry seasons on the availability of soil moisture products. Figure 9 shows the time change of daily average soil moisture and precipitation of representative stations in different climate zones. It can be seen that the feedback effect of soil moisture on precipitation in arid climate zones is weak, which the correlation coefficients of soil moisture and precipitation at Tacheng, Hotan, and Zhangye stations were 0.01, 0.08, and 0.15, respectively. The soil moisture of Zhangye station would fluctuate before and after precipitation, and the soil moisture values of the rest of the two stations are less affected by precipitation and there are hardly characteristics of the same phase as the precipitation. Such a case applies to all four soil moisture products, which may be due to the scarce and concentrated precipitation in the Gobi Desert area while strong solar radiation also leads to greater evaporation [57]. The precipitation in the monsoon-affected zone and the monsoon-affected transition zone has a greater impact on soil moisture and the temporal change trends of soil moisture and precipitation are relatively consistent. This can also be concluded from the correlation coefficients between precipitation and soil moisture (Table not shown). CCI and SMOS products can better capture the dynamic changes in soil moisture at the observation station. If they are consistent with the results of the observation station, the CCI product can give the fluctuation characteristics of the soil moisture at the Yulin station affected by precipitation,

and the SMOS product can reveal the annual continuous precipitation characteristics of the warm season of Haidong station, as well as the continuous drought characteristics of Ulanhot station from September 2019 to March 2020. AMSR2 shows obvious regional differences in terms of precipitation influences. At Haidong station, AMSR2 shows good consistency between soil moisture and precipitation changes, while in Yulin and Beijing stations, the time change trend of soil moisture and precipitation trend are in the opposite phase. These characteristics of a large difference in regional distribution may be related to the aforementioned AMSR2 observation performance under different underlying surface conditions in northern China, which implies that the original AMSR2 product need to be corrected for noise and system error before reasonable application [27,41].

The representativeness of the in situ soil moisture observation has important implications for validation [58,59]. The in situ observation used here is from eight national observation stations in different climate zones. These stations carry out long-term, continuous observation and undertake the task of international and domestic meteorological information exchange. The observation equipment is maintained in time, and the data acquisition is stable and reliable, which can represent the characteristics of climate zoning in a certain range. Further studies are needed to confirm the representativeness of the in situ soil moisture information by statistical methodology [58].

Among the satellite remote-sensing-retrieved products currently released, there is still no set of data that can be recognized as a good description of the distribution and change characteristics of soil moisture in different regions. Therefore, in-depth assessment, preprocessing, and even necessary revisions must be done before using the satellite-retrieved products of soil moisture in order to minimize the estimation bias as much as possible. The preprocessing procedures should be carried out by means of climatological feature analysis, field surveys, and matching of different scales, including issues such as data quality control, data representative evaluation of different depth layers, a judgment of regional representativeness of observation stations using independent data, substitutions of land cover and land types, and carry out corrections based on field observations on these bases [28,60,61]. Of course, the estimation effect of CCI product has indicated that the application of merging multisource observation data is a good way to improve the availability of soil moisture products, which could effectively eliminate the deviation caused by a single instrument on a regional scale [62–64]; for example, the reasonable integration of AMSR2, which was selected for this study to estimate partial wetness in the monsoon region, and SMAP product, which are mainly used for overall estimation of partial dryness, may give a better description of the characteristics of soil moisture distribution in the study area. This is also the work to be carried out in the follow-up of this research. In addition, the spatial resolution of passive microwave-sensor-retrieved soil-moisture products cannot fully meet the needs of business and research. This is also an important problem at present. The continued development of active microwave sensors with high time resolution may be an important direction in the future.

The soil moisture products derived from passive microwave instruments have a high temporal resolution but coarse spatial resolution. To improve their spatial resolution, various downscaling methods have been proposed [65], which use the statistical relationship between soil moisture and factors affecting its distribution, such as the topographic conditions, surface characteristics (land cover, soil texture, and surface temperature), and the climate divisions [66,67]. Validation results in different regions with different types of land cover, soil properties, spatial extent, and climate found that downscaling methods can also ensure better consistency between remote-sensing and in situ observation of soil moisture [68,69]. However, the accuracy of downscaling soil moisture products depends on both the input satellite data and the downscaling method [70]. The applicability of each downscaling method varies widely across different land surface conditions and climate types. There is no single method that can be applied anywhere in the world without any calibration or improvement [66,71]. Many downscaling techniques rely on auxiliary data,

that is, other remote sensing products or geographic information, thus the accuracy of auxiliary data is also critical.

5. Conclusions

Using the daily average observation data of soil moisture on the surface with a depth of 0–10 cm of 1173 stations in northern China from 2019 to 2020, this study compared and analyzed the estimation effects of four satellite microwave sensors including AMSR2, CCI, SMAP, and SMOS, and evaluated the results of soil moisture retrieved products and the applicability of different soil moisture products in the region. The analysis shows that the soil moisture in northern China exhibits obvious regional differences. There is a distribution pattern of "dry in the central and western regions-wet in the east" and "dry in vegetation coverage areas-wet in exposed areas". The areas with lower soil moisture are located in the central regions of northern China while the areas with higher soil moisture are located in the east of Northeast China and primary areas of Shandong.

AMSR2 can give the overall pattern of soil moisture distribution in northern China. The correlation coefficients are characterized as "positive correlation in the monsoon region and negative correlation in the rest of the regions", which is significantly overestimated compared to the actual observations, especially in the eastern monsoon where significant bias towards wetness is found, with larger RMSE between the two products. The probability distributions of soil moisture retrieval of SMAP and SMOS are relatively close to the actual observation, which have positive correlations with the observations, and the retrieval results are better for the dry soil moisture areas in the central and western regions. The results have the satisfactory capability of describing the dry center of soil moisture, but they were predominantly dry. CCI product has the best effect on the description of the soil moisture distribution characteristics in northern China and can give the overall distribution pattern of soil moisture, which is close to the observations and showing significant positive correlations in the area east of 104° E, but there is an overestimation of dry areas and an underestimation of wet areas.

In terms of different seasons, AMSR2 and CCI showed positive deviations for all seasons, and SMAP and SMOS have negative deviations for all seasons. Satellite-retrieved products have the best description ability for summer soil moisture, but poor description ability for winter soil moisture. In general, CCI product gave the best description of soil moisture in spring, summer, and autumn in northern China, while SMAP and SMOS products performed better in winter.

Comparing the distribution characteristics of the deviation of soil moisture products in different climate zones, it can be seen that, for the description of the time changes in soil moisture in arid climate zones, the CCI had a relatively good estimation effect, and the AMSR2 has a good description of the distribution interval of the data. CCI product was relatively effective in estimating soil moisture in the eastern monsoon region, while SMAP and SMOS were poor in availability. In the transition zone affected by the summer monsoon, the availability of the four products in this area was poor. AMSR2 and CCI were mainly overestimated, while the data dispersion of SMAP and SMOS product was the smallest among the three climate zones, but they failed to give the temporal change characteristics of soil moisture. This study suggests that it can be considered as a "good soil moisture retrieval product" with an absolute value of BIAS less than 0.047 (the average value of the absolute value of BIAS of CCI, the optimal product in different seasons), and an RMSE less than 0.092 (the average value of RMSE of CCI in different seasons).

Author Contributions: Conceptualization, W.L.; methodology, W.L., T.X. and J.W.; software, F.X. and C.L.; validation, J.W., T.X. and C.L.; formal analysis, J.W., T.X. and C.L.; investigation, F.X., T.X. and J.W.; data curation, J.W. and F.X.; writing—original draft preparation, W.L.; writing—review and editing, J.W., T.X., F.X. and C.L.; visualization, F.X. and C.L.; supervision, W.L.; project administration, W.L.; funding acquisition, W.L. All authors have read and agreed to the published version of the manuscript.

Funding: This research was funded by National Natural Science Foundation of China, grant number: 41505036, Talent program of Gansu Meteorological Bureau, grant number: 2122rczx-srjh-01 and Innovation Team Project of Gansu Meteorological Bureau, grant No.: GXQXCXTD-2020-01.

Institutional Review Board Statement: Not applicable.

Informed Consent Statement: Not applicable.

Data Availability Statement: In situ observation data of soil moisture and precipitation can be obtained from http://data.cma.cn (accessed on 15 January 2022). AMSR2 datasets are available at https://suzaku.eorc.jaxa.jp/GCOM_W (accessed on 15 January 2022). CCI datasets are available at https://catalogue.ceda.ac.uk/uuid/f5ffbd016e6b44858a33ae38ed2a149e (accessed on 15 January 2022). SMAP datasets are available at https://nsidc.org/data/smap (accessed on 15 January 2022). SMOS datasets are available at https://www.catds.fr/sipad/ (accessed on 5 January 2022).

Acknowledgments: We are grateful to National Meteorological Information Center of China for providing in situ observation data. We thank Yunyun Liu from the National Climate Center of China, and Xiaowei Wang from the Lanzhou Regional Climate Center, for the observation data processing support, and Wei Wang from the Lanzhou Institute of Arid Meteorology, China Meteorological Administration, for the vegetation data processing. We also thank all the editors and reviewers and for their valuable comments and suggestions for improving this manuscript.

Conflicts of Interest: The authors declare no conflict of interest.

References

1. Seneviratne, S.I.; Corti, T.; Davin, E.L.; Hirschi, M.; Jaeger, E.B.; Lehner, I.; Orlowsky, B.; Teuling, A. Investigating soil moisture–climate interactions in a changing climate: A review. *Earth Sci. Rev.* **2010**, *99*, 125–161. [CrossRef]
2. Famiglietti, J.S.; Devereaux, J.A.; Laymon, C.A.; Tsegaye, T.; Houser, P.R.; Jackson, T.J.; Graham, S.T.; Rodell, M.; Oevelen, P.J.V. Ground-based investigation of soil moisture variability within remote sensing footprints During the Southern Great Plains 1997 (SGP97) Hydrology Experiment. *Water Resour. Res.* **2010**, *35*, 1839–1851. [CrossRef]
3. Crow, W.T.; Berg, A.A.; Cosh, M.H.; Loew, A.; Mohanty, B.P.; Panciera, R.; Rosnay, P.D.; Ryu, D.; Walker, J.P. Upscaling sparse ground-based soil moisture observations for the validation of coarse-resolution satellite soil moisture products. *Rev. Geophy.* **2012**, *50*, RG2002. [CrossRef]
4. Su, C.-H.; Narsey, S.; Gruber, A.; Xaver, A.; Chung, D.; Ryu, D.; Wagner, W. Evaluation of post-retrieval de-noising of active and passive microwave satellite soil moisture. *Remote Sens. Environ.* **2015**, *163*, 127–139. [CrossRef]
5. Goward, S.N.; Xue, Y.; Czajkowski, K.P. Evaluating land surface moisture conditions from the remotely sensed temperature/vegetation index measurements: An exploration with the simplified simple biosphere model. *Remote Sens. Environ.* **2002**, *79*, 225–242. [CrossRef]
6. Mallick, K.; Bhattacharya, B.K.; Patel, N.K. Estimating volumetric surface moisture content for cropped soils using a soil wetness index based on surface temperature and NDVI. *Agric. For. Meteorol.* **2009**, *149*, 1327–1342. [CrossRef]
7. Ulaby, F.T.; Dubois, P.C.; Zyl, J. Radar mapping of surface soil moisture. *J. Hydrol.* **1996**, *184*, 57–84. [CrossRef]
8. Kim, S.; Zhang, R.; Pham, H.; Sharma, A. A Review of Satellite-Derived Soil Moisture and Its Usage for Flood Estimation. *Remote Sens. Earth Syst. Sci.* **2019**, *2*, 225–246. [CrossRef]
9. Prigent, C.; Aires, F.; Rossow, W.B.; Robock, A. Sensitivity of satellite microwave and infrared observations to soil moisture at a global scale: 2. Global statistical relationships. *J. Geophys. Res.-Atmos.* **2005**, *110*, D11103. [CrossRef]
10. Pellarin, T.; Calvet, J.-C.; Wagner, W. Evaluation of ERS scatterometer soil moisture products over a half-degree region in southwestern France. *Geophys. Res. Lett.* **2006**, *33*, L17401. [CrossRef]
11. Karthikeyan, L.; Pan, M.; Wandersa, N.; Kumar, D.N.; Wood, E.F. Four decades of microwave satellite soil moisture observations: Part 1. A review of retrieval algorithms. *Adv. Water Resour.* **2017**, *109*, 106–120. [CrossRef]
12. Bindlish, R.; Jackson, T.; Wood, E.; Gao, H.; Starks, P.; Bosch, D.; Lakshmi, V. Soil moisture estimates from TRMM Microwave Imager observations over the Southern United States. *Remote Sens. Environ.* **2003**, *85*, 507–515. [CrossRef]
13. Albergel, C.; Rosnay, P.D.; Gruhier, C.; Muñoz-Sabater, J.; Hasenauer, S.; Isaksen, L.; Kerr, Y.; Wagner, W. Evaluation of remotely sensed and modelled soil moisture products using global ground-based in situ observations. *Remote Sens. Environ.* **2012**, *118*, 215–226. [CrossRef]
14. Parrens, M.; Zakharova, E.; Lafont, S.; Calvet, J.-C.; Kerr, Y.; Wagner, W.; Wigneron, J.-P. Comparing soil moisture retrievals from SMOS and ASCAT over France. *Hydrol. Earth Syst. Sci.* **2012**, *16*, 423–440. [CrossRef]
15. Sahoo, A.K.; Houser, P.R.; Ferguson, C.; Wood, E.F.; Dirmeyer, P.A.; Kafatos, M. Evaluation of AMSR-E soil moisture results using the in-situ data over the Little River Experimental Watershed, Georgia. *Remote Sens. Environ.* **2008**, *112*, 3142–3152. [CrossRef]
16. Draper, C.S.; Walker, J.P.; Steinle, P.J.; Jeu, R.A.M.; Holmes, T.R.H. An evaluation of AMSR-E derived soil moisture over Australia. *Remote Sens. Environ.* **2009**, *113*, 703–710. [CrossRef]

17. An, R.; Zhang, L.; Wang, Z.; Quaye-Ballard, J.A.; You, J.; Shen, X.; Gao, W.; Huang, L.; Zhao, Y.; Ke, Z. Validation of the ESA CCI Soil Moisture Product in China. *Int. J. Appl. Earth Obs. Geoinf.* **2016**, *48*, 28–36. [CrossRef]
18. Karthikeyan, L.; Pan, M.; Wanders, N.; Kumar, D.N.; Wood, E.F. Four Decades of Microwave Satellite Soil Moisture Observations: Part 2. Product Validation and Inter-Satellite Comparisons. *Adv. Water Resour.* **2017**, *109*, 236–252. [CrossRef]
19. Zheng, J.; Zhao, T.; Lü, H.; Shi, J.; Cosh, M.H.; Ji, D.; Jiang, L.; Cui, Q.; Lu, H.; Yang, K.; et al. Assessment of 24 Soil Moisture Datasets Using a New in Situ Network in the Shandian River Basin of China. *Remote Sens. Environ.* **2022**, *271*, 112891. [CrossRef]
20. Parinussa, R.M.; Meesters, A.G.C.A.; Liu, Y.Y.; Dorigo, W.; Wagner, W.; de Jeu, R.A. Error Estimates for Near-Real-Time Satellite Soil Moisture as Derived From the Land Parameter Retrieval Model. *IEEE Geosci. Remote Sens. Lett.* **2011**, *8*, 779–783. [CrossRef]
21. Yuan, S.; Wang, Y.; Quiring, S.M.; Ford, T.W.; Houston, A.L. A sensitivity study on the response of convection initiation to in situ soil moisture in the central United States. *Clim. Dyn.* **2020**, *54*, 2013–2028. [CrossRef]
22. Helgert, S.; Khodayar, S. Improvement of the soil-atmosphere interactions and subsequent heavy precipitation modelling by enhanced initialization using remotely sensed 1 km soil moisture information. *Remote Sens. Environ.* **2020**, *246*, 111812. [CrossRef]
23. Zhang, A.-Z.; Jia, G.-S.; Wang, H.-S.; Zhao, T.-B.; Feng, J.-M.; Ma, Z.-G. Evaluation of AMSR -E-Derived Soil Moisture over Northern China. *Atmos. Ocean. Sci. Lett.* **2011**, *4*, 223–228.
24. Li, Z.; Wang, L.; Wang, L.; Li, X.; Xiao, G. Top-Layer Soil Moisture Retrieval over the Qinghai-Xizang Plateau in Summer Based on AMSR-E Data. *Plateau Meteorol.* **2017**, *36*, 67–78.
25. Zhang, L.; He, C.; Zhang, M.; Zhu, Y. Evaluation of the SMOS and SMAP soil moisture products under different vegetation types against two sparse in situ networks over arid mountainous watersheds, Northwest China. *Sci. China Earth Sci.* **2019**, *62*, 703–718. [CrossRef]
26. Jing, C.L. Comparative evaluation of SMAP & CCI & CLDAS soil moisture products in typical region of Qinghai-Tibet Plateau. *J. Subtrop. Resour. Environ.* **2020**, *15*, 85–94.
27. Cho, E.; Moon, H.; Choi, M. First Assessment of the Advanced Microwave Scanning Radiometer 2 (AMSR2)Soil Moisture Contents in Northeast Asia. *J. Meteor. Soc. Jpn.* **2015**, *93*, 117–129. [CrossRef]
28. Brown, M.E.; Escobar, V.M.; Moran, S.; Entekhabi, D.; O'Neill, P.E.; Njoku, E.G.; Doorn, B.; Entin, J. NASA's Soil Moisture Active Passive (SMAP) Mission and Opportunities for Applications Users. *Bull. Am. Meteorol. Soc.* **2013**, *94*, 1125–1128. [CrossRef]
29. Chan, S.K.; Bindlish, R.; O'Neill, P.; Jackson, T.; Njoku, E.; Dunbar, S.; Chaubell, J.; Piepmeier, J.R.; Yueh, S.; Entekhabi, D.; et al. Development and assessment of the SMAP enhanced passive soil moisture product. *Remote Sens. Environ.* **2018**, *204*, 931–941. [CrossRef]
30. Louvet, S.; Pellarin, T.; Bitar, A.A.; Cappelaere, B.; Galle, S.; Manuela, G.; Gruhier, C.; Kerr, Y.; Lebel, T.; Mialon, A.; et al. SMOS soil moisture product evaluation over West-Africa from local to regional scale. *Remote Sens. Environ.* **2015**, *156*, 383–394. [CrossRef]
31. González-Zamora, Á.; Sánchez, N.; Pablos, M.; Martínez-Fernández, J. CCI soil moisture assessment with SMOS soil moisture and in situ data under different environmental conditions and spatial scales in Spain. *Remote Sens. Environ.* **2019**, *225*, 469–482. [CrossRef]
32. Dorigo, W.; Wagner, W.; Albergel, C.; Albrecht, F.; Balsamo, G.; Brocca, L.; Chung, D.; Ertl, M.; Forkel, M.; Gruber, A.; et al. ESA CCI Soil Moisture for improved Earth system understanding: State-of-the art and future directions. *Remote Sens. Environ.* **2017**, *203*, 185–215. [CrossRef]
33. Gruber, A.; Scanlon, T.; Schalie, R.V.D.; Wagner, W. Evolution of the ESA CCI Soil Moisture climate data records and their underlying merging methodology. *Earth Syst. Sci. Data* **2019**, *11*, 717–739. [CrossRef]
34. Su, B.; Wang, A.; Wang, G.; Wang, Y.; Jiang, T. Spatiotemporal Variations of Soil Moisture in the Tarim River Basin, China. *Int. J. Appl. Earth Obs. Geoinf.* **2016**, *48*, 122–130. [CrossRef]
35. Wang, Y.; Yang, J.; Chen, Y.; Wang, A.; De Maeyer, P. The Spatiotemporal Response of Soil Moisture to Precipitation and Temperature Changes in an Arid Region, China. *Remote Sens.* **2018**, *10*, 468. [CrossRef]
36. Phadia, E.G. Minimax Estimation of a Cumulative Distribution Function. *Ann. Stat.* **1973**, *1*, 1149–1157. [CrossRef]
37. Hyndman, R.; Koehler, A. Another look at measures of forecast accuracy. *Int. J. Forecast.* **2006**, *22*, 679–688. [CrossRef]
38. Taylor, K.E. Summarizing multiple aspects of model performance in a single diagram. *J. Geophys. Res.-Atmos.* **2001**, *106*, 7183–7192. [CrossRef]
39. Zhuang, Y.; Shi, C.; Shen, R.; Jiang, L.; Wang, S. Quality Evaluation of Multi-Microwave Remote Sensing Soil Moisture Products over China. *J. Meteorol. Sci.* **2015**, *35*, 289–296.
40. Liu, W.; Zhang, Q.; Fu, Z. Variation Characteristics of Precipitation and Its Affecting Factors in Northwest China over the Past 55 Years. *Plateau Meteorol.* **2017**, *36*, 1533–1545.
41. Peng, J.; Niesel, J.; Loew, A.; Zhang, S.; Wang, J. Evaluation of satellite and reanalysis soil moisture products over Southwest China using ground-based measurements. *Remote Sens.* **2015**, *7*, 15729–15747. [CrossRef]
42. Gruhier, C.; Rosnay, P.D.; Hasenauer, S.; Holmes, T.R.H.; Jeu, R.D.; Kerr, Y.; Mougin, E.; Njoku, E.G.; Timouk, F.; Wagner, W.; et al. Soil moisture active and passive microwave products: Intercomparison and evaluation over a Sahelian site. *Hydrol. Earth Syst. Sci.* **2010**, *14*, 141–156. [CrossRef]
43. Miralles, D.; Crow, W.; Cosh, M.H. Estimating spatial sampling errors in coarse-scale soil moisture estimates derived from point-scale observations. *J. Hydrometeorol.* **2010**, *11*, 1423–1429. [CrossRef]
44. Hain, C.R.; Crow, W.T.; Mecikalski, J.R.; Anderson, M.C.; Holmes, T. An intercomparison of available soil moisture estimates from thermal infrared and passive microwave remote sensing and land surface modeling. *J. Geophys. Res.-Atmos.* **2011**, *116*, D15107. [CrossRef]

45. Isla, T.; Srivastava, P.K.; Dai, Q.; Gupta, M.; Zhuo, L. An introduction to factor analysis for radio frequency interference detection on satellite observations. *Meteorol. Appl.* **2015**, *22*, 436–443. [CrossRef]
46. Srivastava, P.K. Satellite Soil Moisture: Review of Theory and Applications in Water Resources. *Water Resour. Manag.* **2017**, *31*, 3161–3176. [CrossRef]
47. Mecklenburg, S.; Drusch, M.; Kerr, Y.; Martin-Neira, M.; Steven, D.; Buenadicha, G.; Reul, N.; Daganzo, E.; Oliva, R.; Crapolicchio, R. ESA's soil moisture and ocean salinity mission: Mission performance and operations. *IEEE Trans. Geosci. Remote* **2012**, *50*, 1354–1366. [CrossRef]
48. Aksoy, M.; Johnson, J.T. A study of SMOS RFI over North America. *IEEE Geosci. Remote. Sens. Lett.* **2013**, *10*, 515–519. [CrossRef]
49. Spencer, M.W.; Chen, C.W.; Ghaemi, H.; Chan, S.F.; Belz, J.E. RFI characterization and mitigation for the SMAP radar. *IEEE Tran. Geosci. Remote* **2013**, *51*, 4973–4982. [CrossRef]
50. Piepmeier, J.R.; Johnson, J.T.; Mohammed, P.; Bradley, D.; Ruf, C.; Aksoy, M.; García, R.; Hudson, D.; Miles, L.; Wong, M. Radio-frequency interference mitigation for the soil moisture active passive microwave radiometer. *IEEE Trans. Geosci. Remote* **2014**, *52*, 761–775. [CrossRef]
51. Sawada, Y.; Tsutsui, H.; Koike, T.; Rasmy, M.; Fujii, H. A Field Verification of an Algorithm for Retrieving Vegetation Water Content From Passive Microwave Observations. *IEEE Trans. Geosci. Remote Sens.* **2015**, *54*, 2082–2095. [CrossRef]
52. Zwieback, S.; Colliander, A.; Cosh, M.H.; Martínez-Fernández, J.; McNairn, H.; Starks, P.; Thibeault, M.; Berg, A. Estimating time-dependent vegetation biases in the SMAP soil moisture product. Hydrol. *Earth Syst. Sci.* **2018**, *22*, 4473–4489. [CrossRef]
53. Wang, A.; Zeng, X. Evaluation of multireanalysis products with in situ observations over the Tibetan Plateau. *J. Geophys. Res.-Atmos.* **2012**, *117*, d05102. [CrossRef]
54. Leroux, D.J.; Kerr, Y.H.; Richaume, P.; Fieuzal, R. Spatial distribution and possible sources of SMOS errors at the global scale. *Remote Sens. Environ.* **2013**, *13*, 240–250. [CrossRef]
55. Yee, M.S.; Walker, J.P.; Rüdiger, C.; Parinuss, R.M.; Koike, T.; Kerr, Y.H. A comparison of SMOS and AMSR2 soil moisture using representative sites of the OzNet monitoring network. *Remote Sens. Environ.* **2017**, *195*, 297–312. [CrossRef]
56. McColl, K.A.; Alemohammad, S.H.; Akbar, R.; Konings, A.G.; Yueh, S.; Entekhabi, D. The global distribution and dynamics of surface soil moisture. *Nat. Geosci.* **2017**, *10*, 100–104. [CrossRef]
57. Liu, W.; Fu, Z.; Chen, X.; Qu, J.; Wang, J.; Peng, X. Inhomogeneity of precipitation and its influencing factors in Northwest China from 1961 to 2015. Theor. *Appl. Clim.* **2019**, *138*, 1831–1844. [CrossRef]
58. Gruber, A.; Lannoy, G.D.; Albergel, C.; Al-Yaari, A.; Wagner, W. Validation Practices for Satellite Soil Moisture Retrievals: What Are (the) Errors? *Remote Sens. Environ.* **2020**, *244*, 111806. [CrossRef]
59. Dorigo, W.; Himmelbauer, I.; Aberer, D.; Schremmer, L.; Petrakovic, I.; Zappa, L.; Preimesberger, W.; Xaver, A.; Annor, F.; Ardö, J.; et al. The International Soil Moisture Network: Serving Earth System Science for over a Decade. *Hydrol. Earth Syst. Sci.* **2021**, *25*, 5749–5804. [CrossRef]
60. Sutanudjaja, E.H.; Van Beek, L.P.; De Jong, S.M.; Van Geer, F.C.; Bierkens, M.F. Calibrating a large-extent high-resolution coupled groundwater-land surface model using soil moisture and discharge data. *Water Resour. Res.* **2014**, *50*, 687–705. [CrossRef]
61. Enenkel, M.; Reimer, C.; Dorigo, W.; Wagner, W.; Pfeil, I.; Parinussa, R.; Jeu, R.D. Combining satellite observations to develop a global soil moisture product for near-real-time applications. *Hydrol. Earth Syst. Sci.* **2016**, *20*, 4191–4208. [CrossRef]
62. Liu, Y.Y.; Dorigo, W.A.; Parinussa, R.M.; de Jeu, R.A.; Wagner, W.; McCabe, M.F.; Evans, J.P.; Van Dijk, A.I. Trend-preserving blending of passive and active microwave soil moisture retrievals. *Remote Sens. Environ.* **2012**, *123*, 280–297. [CrossRef]
63. Cheng, M.; Zhong, L.; Ma, Y.; Zou, M.; Ge, N.; Wang, X.; Hu, Y. A study on the assessment of multi-source satellite soil moisture products and reanalysis data for the Tibetan Plateau. *Remote Sens.* **2019**, *11*, 1196. [CrossRef]
64. Jiang, H.; Shen, H.; Li, X.; Zeng, C.; Liu, H.; Lei, F. Extending the SMAP 9-km soil moisture product using a spatio-temporal fusion model. *Remote Sens. Environ.* **2019**, *231*, 111224.
65. Peng, J.; Loew, A.; Merlin, O.; Verhoest, N. A review of spatial downscaling of satellite remotely sensed soil moisture. *Rev. Geophys.* **2017**, *55*, 341–366. [CrossRef]
66. Deshon, J.; Niemann, J.; Green, T.; Jones, A.; Grazaitis, P. Stochastic analysis and probabilistic downscaling of soil moisture in small catchments. *J. Hydrol.* **2020**, *585*, 124711. [CrossRef]
67. Xu, C.; Qu, J.J.; Hao, X.; Cosh, M.H.; Prueger, J.H.; Zhu, Z.; Gutenberg, L. Downscaling of Surface Soil Moisture Retrieval by Combining MODIS/Landsat and In Situ Measurements. *Remote Sens.* **2018**, *10*, 210. [CrossRef]
68. Verhoest, N.; van den Berg, M.; Martens, B.; Lievens, H.; Wood, E.; Pan, M.; Kerr, Y.; Bitar, A.; Tomer, S.; Drusch, M.; et al. Copula-Based Downscaling of Coarse-Scale Soil Moisture Observations With Implicit Bias Correction. *IEEE Trans. Geosci. Remote Sens.* **2015**, *53*, 3507–3521. [CrossRef]
69. Montzka, C.; Rötzer, K.; Bogena, H.R.; Sanchez, N.; Vereecken, H. A New Soil Moisture Downscaling Approach for SMAP, SMOS, and ASCAT by Predicting Sub-Grid Variability. *Remote Sens.* **2018**, *10*, 427. [CrossRef]
70. Das, N.; Entekhabi, D.; Dunbar, R.; Njoku, E.; Yueh, S. Uncertainty estimates in the SMAP combined active-passive downscaled brightness temperature. *IEEE Trans. Geosci. Remote Sens.* **2016**, *54*, 640–650. [CrossRef]
71. Walker, J.; Houser, P. Requirements of a global near-surface soil moisture satellite mission: Accuracy, repeat time, and spatial resolution. *Adv. Water Resour.* **2004**, *27*, 785–801. [CrossRef]